

Singlet State *Cis,Trans* Photoisomerization and Intersystem Crossing of 1-Arylpropenes

Frederick D. Lewis,* Dario M. Bassani, Richard A. Caldwell,* and David J. Unett

Contribution from the Departments of Chemistry, Northwestern University, Evanston, Illinois 60208-3113, and The University of Texas at Dallas, Richardson, Texas 75083

Received July 12, 1994[⊗]

Abstract: The temperature dependence of the singlet state lifetime and photoisomerization and fluorescence quantum yields for *trans*- and *cis*-1-phenylpropene have been determined in hexane solution. Calculated barriers for twisting about the double bond on the singlet potential energy surface are 8.8 and 4.6 kcal/mol for the *trans* and *cis* isomer, respectively. The barrier for the *trans* isomer is sufficiently high to prevent isomerization on the singlet state surface at or below room temperature. However, isomerization occurs at low temperatures as a consequence of intersystem crossing to the triplet state, which undergoes barrierless isomerization. The quantum yield for intersystem crossing, as determined by time-resolved photoacoustic calorimetry, is 0.60 ± 0.03 and the rate constant for intersystem crossing is $4.7 \times 10^7 \text{ s}^{-1}$. While internal conversion is not significant at or below room temperature, thermally activated internal conversion competes with singlet isomerization at high temperatures. The *cis* isomer undergoes isomerization predominantly via the singlet state at room temperature. Both electron-donating (*p*-methoxy) and electron-withdrawing (*m*- and *p*-cyano, *p*-carbomethoxy, and *p*-trifluoromethyl) aromatic substituents are found to lower the barrier for singlet state isomerization. Increased solvent polarity (acetonitrile vs hexane) results in variable decreases in the barrier for singlet state isomerization. Photoisomerization of the *p*-cyano derivative at room temperature occurs predominantly via the triplet state in hexane solution and via the singlet state in acetonitrile solution. The effects of substituents and solvent are better correlated with the magnitude of the S_2-S_1 energy gap than the stability of either zwitterionic or biradical intermediates. Rate constants for intersystem crossing are, in most cases, not highly dependent upon aromatic substitution or solvent polarity.

Introduction

The behavior of the lowest electronically excited states of conjugated olefins has attracted the attention of photochemists, spectroscopists, and theoreticians, interested in elucidating the mechanism of double-bond photoisomerization. *cis*- and *trans*-stilbene (*c*-S and *t*-S) and their derivatives have been the subject of numerous investigations, and the nature of the stilbene excited singlet state and triplet state potential energy surfaces is understood in considerable detail.^{1,2} In comparison, relatively little is known about the styrene excited singlet state potential energy surface, in spite of numerous spectroscopic^{3–9} and theoretical^{10–14} investigations of the styrene singlet state. Photoisomerization cannot be experimentally investigated in

styrene; however, both its β -deuterio³ and β -methyl derivatives^{15,16} are reported to undergo photoisomerization. While there have been suggestions that styrene can undergo twisting about its ethylenic bond on the singlet surface, current evidence indicates that the barrier for such twisting is too large to permit isomerization at room temperature. Several calculations of the styrene potential energy surface have resulted in values ranging from 4 to 25 kcal/mol for this barrier.^{11–14}

The substantially longer singlet lifetime for styrene vs *t*-S (14.8 vs 0.1 ns) permits intersystem crossing to compete with other singlet decay pathways for styrene, whereas intersystem crossing in not a significant decay pathway for *t*-S. Low quantum yields for intersystem crossing were reported by Zimmerman et al.¹⁷ for several phenylalkenes ($\Phi_{st} \leq 0.11$). Some years later Bonneau¹⁸ reported a value of $\Phi_{st} = 0.40$ for styrene and lower values ($\Phi_{st} \leq 0.14$) for several phenylalkenes and phenylcycloalkenes. In contrast to the styrene excited singlet potential energy surface, the styrene triplet potential energy surface has been thoroughly investigated by Caldwell and co-workers¹⁹ and by Tokumaru and co-workers.²⁰ The triplet states of *trans*-1-phenylpropene (*t*-1) and *cis*-1-phenyl-

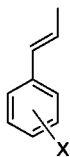
[⊗] Abstract published in *Advance ACS Abstracts*, October 1, 1994.
 (1) Saitli, J.; Sun, Y.-P. In *Photochromism, Molecules and Systems*; Dürr, H., Bouais-Laurent, H., Eds.; Elsevier: Amsterdam, 1990; p 64.
 (2) Waldeck, D. H. *Chem. Rev.* **1991**, *91*, 415.
 (3) Hui, M. H.; Rice, S. A. *J. Chem. Phys.* **1974**, *61*, 833.
 (4) Ghiggino, K. P.; Hara, K.; Salisbury, K.; Phillips, D. J. *Chem. Soc., Faraday Trans. 2* **1978**, 607.
 (5) Lyons, A. L., Jr.; Turro, N. J. *J. Am. Chem. Soc.* **1978**, *100*, 3177.
 (6) Condirston, D. A.; Lapos, J. D. *Chem. Phys. Lett.* **1979**, *63*, 313.
 (7) Leopold, D. G.; Hemley, R. J.; Vaida, V.; Roebber, J. L. *J. Chem. Phys.* **1981**, *75*, 4758.
 (8) Syage, J. A.; Al Adel, F.; Zewail, A. H. *Chem. Phys. Lett.* **1983**, *103*, 15.
 (9) Grassian, V. H.; Bernstein, E. R.; Secor, H. V.; Seeman, J. I. *J. Phys. Chem.* **1989**, *93*, 3470.
 (10) Fueno, T.; Yamaguchi, K.; Naka, Y. *Bull. Chem. Soc. Jpn.* **1972**, *45*, 3294.
 (11) Bruni, M. C.; Momicchioli, F.; Baraldi, I. *Chem. Phys. Lett.* **1975**, *36*, 484.
 (12) (a) Orlandi, G.; Palmieri, P.; Poggi, G. *J. Chem. Soc., Faraday Trans. 2* **1981**, *77*, 71. (b) Michl, J.; Bonacic-Koutecky, V. *Electronic Aspects of Organic Photochemistry*; Wiley-Interscience: New York, 1990; p 310.
 (13) Said, M.; Malrieu, J.-P. *Chem. Phys. Lett.* **1983**, *102*, 312.

(14) Hemley, R. J.; Dinur, U.; Vaida, V.; Karplus, M. *J. Am. Chem. Soc.* **1985**, *107*, 836.
 (15) (a) Rockley, M. G.; Salisbury, K. *J. Chem. Soc., Perkins Trans. 2* **1973**, *69*, 1582. (b) Crosby, P. M.; Salisbury, K. *J. Chem. Soc., Chem. Commun.* **1975**, 477.
 (16) Lewis, F. D.; Bassani, D. M. *J. Am. Chem. Soc.* **1993**, *115*, 7523.
 (17) Zimmerman, H. E.; Kamm, K. S.; Werthemann, D. P. *J. Am. Chem. Soc.* **1974**, *96*, 7821.
 (18) Bonneau, R. *J. Am. Chem. Soc.* **1982**, *104*, 2921.
 (19) Caldwell, R. A.; Sovocool, G. W.; Peresie, R. J. *J. Am. Chem. Soc.* **1973**, *95*, 1496. (b) Ni, T.; Caldwell, R. A.; Melton, L. A. *J. Am. Chem. Soc.* **1989**, *111*, 457.
 (20) Arai, T.; Sakuragi, H.; Tokumaru, K. *Bull. Chem. Soc. Jpn.* **1982**, *55*, 2204.

propene (*c*-1) are reported to undergo essentially activationless isomerization with quantum yields of 0.5, as expected for a perpendicular triplet which decays with equal probability to ground state *t*-1 and *c*-1.

Salisbury and co-workers¹⁵ have investigated the room temperature fluorescence and photoisomerization of *trans*-1-phenylpropene (*t*-1) and *cis*-1-phenylpropene (*c*-1) both in the vapor phase and in solution. They concluded that isomerization occurs via intersystem crossing and that the barrier to twisting on the singlet state surface is sufficiently large (>10 kcal/mol) to prevent isomerization. We recently reported the results of an investigation of the temperature dependence of the singlet lifetimes and isomerization quantum yields of *t*-1 and *c*-1 in hexane solution over an extended temperature range.¹⁶ Analysis of these data indicated that the barriers for isomerization on the singlet state surfaces of *t*-1 and *c*-1 are 8.8 and 4.6 kcal/mol, respectively. As a consequence of these different barriers, isomerization of *t*-1 at room temperature occurs predominantly via intersystem crossing, as earlier suggested by Salisbury and co-workers,¹⁵ whereas isomerization of *c*-1 occurs predominantly via the singlet state.

In addition to uncertainty over the barrier height for styrene singlet state isomerization, there has been disagreement as to the nature of the lowest twisted singlet state. Both zwitterionic (hole-pair)¹² and diradical¹³ lowest twisted singlet states have been proposed by different groups of theoreticians. If the transition state for twisting on the singlet surface resembles the twisted singlet, investigation of the effects of aromatic substituents and solvent polarity on the height of the singlet barrier might provide information about the nature of the twisted singlet. We report here the results of our investigation of the effects of temperature upon the fluorescence and photoisomerization of the 1-arylpropenes *t*-1-*t*-6 and *c*-1 in hexane and acetonitrile solution. Both aryl substituents and solvent polarity are found to influence the barrier for singlet state isomerization and hence the competition between singlet and triplet isomerization pathways. However, analysis of the Arrhenius parameters does not support a polar transition state for singlet state isomerization. Rate constants for intersystem crossing and fluorescence are independent of temperature whereas internal conversion is temperature dependent and appears to be related to the singlet isomerization process. We have also determined the quantum yield for intersystem crossing in *t*-1 by means of time-resolved photoacoustic calorimetry and find a significantly higher value than that previously reported for styrene and phenylalkenes.



- t*-1: X = H
t-2: X = *p*-CN
t-3: X = *m*-CN
t-4: X = *p*-CO₂CH₃
t-5: X = *p*-CF₃
t-6: X = *p*-OCH₃

Results

Electronic Spectra. The absorption spectra of *c*-1 and *t*-1 through *t*-6²¹ resemble that of styrene,¹⁰ consisting of a weak long-wavelength absorption band which displays some vibrational structure and a stronger, structureless band at higher energy. The wavelengths of the first maxima in the long-

Table 1. Observed Absorption Maxima and Results of INDO/S CI Calculations for the Electronic Transitions of Substituted 1-Arylpropenes

| transition | energy | | | description |
|-------------|----------------|------------|--------------|--|
| | obs (nm) | calcd (nm) | osc str (au) | |
| <i>c</i> -1 | S ₁ | 288 | | |
| | S ₂ | 256 | | |
| <i>t</i> -1 | S ₁ | 284 | 284 | 0.008 0.34 [22-24] + 0.56 [23-25] |
| | S ₂ | 250 | 260 | 0.700 [23-24] |
| <i>t</i> -2 | S ₁ | 300 | 287 | 0.002 0.42 [26-28] + 0.50 [27-29] |
| | S ₂ | 268 | 263 | 0.814 [27-28] |
| <i>t</i> -3 | S ₁ | 298 | 291 | 0.009 0.25 [26-28] + 0.40 [27-29] + 0.16 [27-28] |
| | S ₂ | 254 | 248 | 0.553 [27-28] |
| <i>t</i> -4 | S ₁ | 300 | 294 | 0.004 0.45 [33-35] + 0.40 [34-36] |
| | S ₂ | 274 | 281 | 0.763 [34-35] |
| <i>t</i> -6 | S ₁ | 298 | 288 | 0.016 0.29 [28-30] + 0.62 [29-31] |
| | S ₂ | 260 | 252 | 0.695 [29-30] |

wavelength bands and the maximum of the higher energy bands in hexane solution are reported in Table 1. Substituents shift both maxima to lower energy compared to *t*-1. The maxima of *c*-1 are at higher energy compared to *t*-1. In the more polar solvent acetonitrile the higher energy band is broadened, in some cases virtually obscuring the lower energy band. However, the band maxima show only minor solvent shifts (0–4 nm).

In order to obtain further information about the effects of aryl substituents on the electronic structure and absorption spectra of these molecules, we have performed INDO/S-SCF-CI (ZINDO)²² calculations for several of the *trans*-1-arylpropenes. ZINDO calculations were not performed for *t*-5 due to the absence of accurate parameters for trifluoromethyl-substituted aromatics. The calculated energies and oscillator strengths for the two lowest energy singlet transitions and major configurations contributing to these transitions are reported in Table 1. In all cases it was found that the lowest energy transition possesses a low oscillator strength and can be described as a combination of the HOMO → (LUMO + 1) and (HOMO - 1) → LUMO. The strongly allowed transition at higher energies can be described as a pure HOMO to LUMO transition. The molecular orbitals involved for *t*-1 are depicted graphically in Figure 1. The relative magnitudes of the coefficients for three highest occupied and three lowest unoccupied molecular orbitals of *t*-1 are shown in Figure 1. The appearance of the frontier orbitals for the other 1-arylpropenes is similar to those for *t*-1. The presence of substituents does not result in a change in the nature of the MO's involved in the two lowest energy transitions.

The fluorescence spectra of the 1-arylpropenes²¹ display either two maxima or a high-energy shoulder and a single maximum in hexane solution. The wavelengths of the high-energy maxima or shoulders in hexane and acetonitrile solution are summarized in Table 2. As is the case for the absorption maxima, aryl substituents shift the fluorescence maxima to lower energy whereas increased solvent polarity (acetonitrile vs hexane) leads to broadening of the fluorescence but has little influence on the fluorescence maxima (0–3 nm shifts). No phosphorescence was observed from any of the 1-arylpropenes either at room temperature or when cooled to 77 K in a methylcyclohexane glass.

Fluorescence quantum yields were determined at room temperature in dilute (<10⁻³ M) deoxygenated hexane solution

(22) (a) Bacon, A. D.; Zerner, M. C. *Theor. Chim. Acta* **1979**, *53*, 21. (b) Zerner, M. C.; Loew, G. H.; Kirchner, R. F.; Mueller-Westernhoff, U. *T. J. Am. Chem. Soc.* **1980**, *102*, 589.

(21) Available as supplementary material.

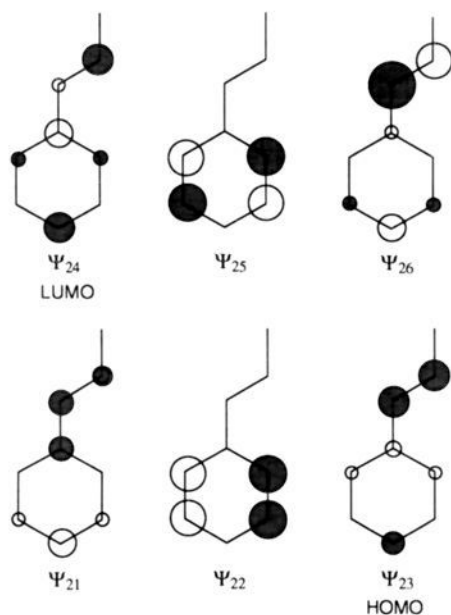


Figure 1. Frontier orbitals involved in the first two electronic transitions of *trans*-1-phenylpropene.

Table 2. Photophysical Data for the 1-Arylpropenes in Hexane and Acetonitrile Solution at Room Temperature

| | solvent | λ_{em} , nm | τ_s , ^a ns | Φ_f ^b | $10^{-7}k_f$, s ⁻¹ | Φ_f ^c |
|-------------|--------------|---------------------|----------------------------|-----------------------|--------------------------------|-----------------------|
| <i>c</i> -1 | hexane | 306 | 2.6 | 0.03 (0.02) | 1.2 | 0.14 (0.20) |
| | acetonitrile | 306 | 2.2 | | | 0.14 |
| <i>t</i> -1 | hexane | 308 | 11.8 (12.7) | 0.35 (0.30) | 3.0 | 0.12 (0.20) |
| | acetonitrile | 307 | 10.9 | | | 0.17 |
| <i>t</i> -2 | hexane | 315 | 5.5 | 0.32 (0.15) | 5.8 | 0.08 (0.12) |
| | acetonitrile | 314 | 0.4 | | | 0.34 |
| <i>t</i> -3 | hexane | 328 | 9.5 | 0.21 (0.26) | 2.2 | 0.20 (0.15) |
| | acetonitrile | 326 | 11.3 | | | 0.27 |
| <i>t</i> -4 | hexane | 315 | 0.8 | 0.05 (0.03) | 6.3 | 0.33 (0.33) |
| | acetonitrile | 317 | 0.5 | | | 0.30 |
| <i>t</i> -5 | hexane | 306 | 3.5 | 0.15 (0.09) | 4.2 | 0.25 (0.23) |
| | acetonitrile | 306 | 2.6 | | | 0.26 |
| <i>t</i> -6 | hexane | 322 | 8.5 | 0.42 (0.38) | 4.9 | 0.12 (0.20) |
| | acetonitrile | 325 | 7.2 | | | 0.13 |

^a Values for 10^{-3} M 1-arylpropene or extrapolated to zero concentration (value in parentheses). ^b Values for excitation of 1-arylpropenes ($\leq 10^{-3}$ M) into S_1 or S_2 (data in parentheses). ^c Values for excitation of 10^{-2} M 1-arylpropene at 281 or 254 nm (data in parentheses).

using styrene ($\Phi_f = 0.24^6$) as a secondary standard. Data for excitation into both the first and second absorption bands are summarized in Table 2. Values of Φ_f are highly dependent upon substituent, varying from 0.42 for *t*-6 to 0.05 for *t*-4 and 0.03 for *c*-1. Values of Φ_f are also excitation wavelength dependent, displaying lower values for S_2 vs S_1 excitation, except in the case of *t*-3. Fluorescence decay times (τ_s) were measured at room temperature in both hexane and acetonitrile solution by time-correlated single photon counting and are reported in Table 2. Good fits to single exponential decays were obtained in all cases for excitation into either S_1 or S_2 . The singlet lifetimes are highly dependent upon substituent, but they display only minor dependence upon solvent polarity, except in the case of *t*-2. Fluorescence quantum yields (S_1 excitation) and lifetimes were measured in hexane solution at several temperatures in the range 220–300 K. Data for *t*-1 are reported in Table 3 while data for the other 1-arylpropenes are available as supplementary material. The values of both Φ_f and τ_s increase with decreasing temperature, resulting in temperature-independent values for the fluorescence rate constant ($k_f = \Phi_f \tau_s^{-1}$). As previously noted for styrene⁶ and *t*-6,²³

Table 3. Temperature Dependence of the Singlet Lifetime and Quantum Yields for Fluorescence and Isomerization of *trans*-1-Phenylpropene^a

| <i>T</i> (K) | hexane | | | acetonitrile | |
|--------------|-------------|----------|----------|--------------|----------|
| | τ (ns) | Φ_f | Φ_i | τ (ns) | Φ_f |
| 473 | 0.98 | 0.12 | | | |
| 453 | 1.42 | 0.13 | | | |
| 433 | 1.97 | 0.14 | | | |
| 413 | 2.76 | 0.14 | | 2.63 | 0.31 |
| 393 | 3.59 | 0.15 | | 4.15 | 0.29 |
| 373 | | | | 5.50 | 0.25 |
| 353 | | | | 6.28 | 0.24 |
| 340 | | | | 8.85 | 0.19 |
| 320 | | | | 10.3 | 0.21 |
| 300 | 11.6 | 0.13 | 0.30 | 8.14 | 0.17 |
| 280 | 12.1 | 0.14 | 0.30 | 11.6 | 0.15 |
| 260 | 12.5 | 0.13 | 0.31 | 11.8 | 0.15 |
| 240 | 12.8 | 0.13 | 0.32 | | |
| 230 | | | | 12.2 | 0.12 |
| 220 | 13.2 | 0.14 | 0.32 | | |

^a Deoxygenated hexane or acetonitrile solution, excitation at 281 nm.

the singlet lifetime of *t*-1 is concentration dependent. A Stern–Volmer plot of the lifetime data determined at several concentrations (0.001–0.02 M) provides values of $\tau_s^0 = 12.7$ ns and the rate constant for self-quenching of $k_{sq} = 7.5 \times 10^9$ M⁻¹ s⁻¹.

Photoisomerization. Quantum yields for photoisomerization were determined at low conversions of reactant isomer (<5% as determined by GC) using either 254 or 281 nm excitation. Optically dense solutions (ca. 10^{-2} M) were employed to assure complete absorption of the incident light. Isomerization quantum yields measured at room temperature are reported in Table 2. While isomerization is the major photoprocess for all of the styrenes investigated, photodimerization also occurs under these conditions. In the case of 10^{-2} M *t*-6 the quantum yields for isomerization and dimerization are 0.12 and 0.015, respectively.²³ In the case of *t*-1 several products tentatively identified as cyclodimers were detected by GC/MS. The sum of the integrated areas for these dimers is comparable to that for *c*-1 formation. Dimer formation competes less effectively with isomerization for the other 1-arylpropenes. Quantum yields for photoisomerization are dependent upon substituent, solvent, and excitation wavelength. Irradiation at 254 nm results in selective S_2 excitation for all of the 1-arylpropenes. Irradiation at 281 nm results in selective excitation of S_1 except in the case of *t*-2 and *t*-4 for which excitation occurs in the red edge of the S_2 band. Quantum yields for isomerization and singlet lifetimes were measured in hexane and acetonitrile solution over a range of temperatures (220–300 K for *c*-1, *t*-4, and *t*-5 and 220–473 K for *t*-1–*t*-3 and *t*-6). Data for *t*-1 are reported in Table 3 while data for the other 1-arylpropenes are available as supplementary material.

Photoacoustic Measurements. Intersystem crossing of singlet *t*-1 was investigated by means of photoacoustic calorimetry. Details of the experimental technique, cell design, and data analysis have been published.^{19b,24} Representative photoacoustic waveforms following 266 nm excitation of optically matched solutions of *t*-1 (1.435 mM, E-Wave) and the reference compound 2-hydroxybenzophenone (T-Wave) in deoxygenated cyclohexane solution are shown in Figure 2. Waveforms are the average of 50 pulses with an incident power approximately 100 μ J per pulse. Less than 5% of the sample is excited under these conditions. The waveforms are deconvoluted assuming

(23) Lewis, F. D.; Kojima, M. *J. Am. Chem. Soc.* **1988**, *110*, 8660.

(24) (a) Melton, L. A.; Ni, T.; Lu, Q. *Rev. Sci. Instrum.* **1989**, *60*, 3217. (b) Arnaut, L. G.; Caldwell, R. A.; Elbert, J. E.; Melton, L. A. *Rev. Sci. Instrum.* **1992**, *63*, 5381.

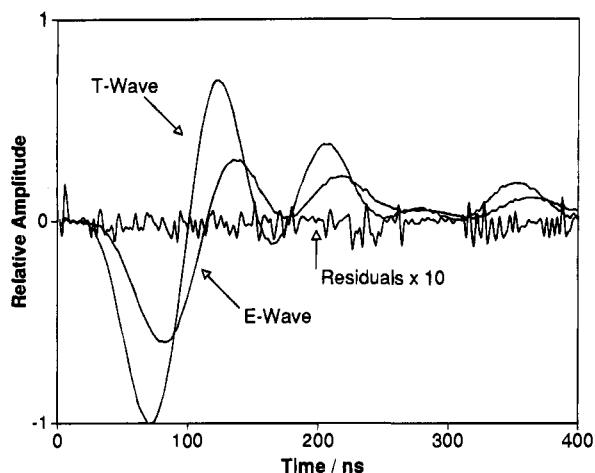


Figure 2. Representative photoacoustic waveforms following 266 nm excitation of optically matched solutions of *trans*-1-phenylpropene (1.435 mM, E-Wave) and 2-hydroxybenzophenone (T-Wave) in cyclohexane. Waveforms are the average of 50 pulses. Incident power approximately 100 μJ per pulse.

three sequential heat decays, each characterized by a decay rate (τ_n) and the fraction of photon energy released (ϕ_n). The first is generation of singlet *t*-1, with fixed values of $\tau_1 = 0.1$ ns (assumed to be faster than the 1 ns transducer resolution) and $\phi_1 = 0.0882$ (calculated from the *t*-1 singlet energy and incident photon energy). The second is singlet decay, for which a value of $\tau_2 = 11.8$ ns is available (Table 2). The third is triplet decay, for which a value of $\tau_3 = 27.0$ ns has been reported.^{19b,25} A six parameter fitting routine was employed in all data analyses in which τ_1 and ϕ_1 were fixed along with τ_2 , or τ_3 , or both. Similar calculated values of ϕ_3 are obtained when all three lifetimes are fixed or when either the singlet or triplet lifetime is allowed to float. The values of τ_2 and τ_3 calculated when one is allowed to float are within experimental error of the measured values. The calculated values of ϕ_3 decrease with increasing *t*-1 concentration but are independent of laser power (50–500 μJ per pulse).

Analysis of the concentration dependence of ϕ_3 provides a limiting value of $\phi_3^0 = 0.284 \pm 0.015$ with a confidence limit of 90% and a value of $k_{sq} = 6 \pm 2 \times 10^9 \text{ M}^{-1} \text{ s}^{-1}$, in good agreement with the value determined from singlet lifetime measurements. The quantum yield for intersystem crossing Φ_{st} is related to ϕ_3 as shown in eq 1,

$$\Phi_{st} = \phi_3^0 E_{hv} E_T \quad (1)$$

where E_{hv} is the photon energy and E_T is the relaxed triplet energy of *t*-1 (corrected for decay to a 50/50 mixture of the *trans* and *cis* ground states, where the *c*-1 ground state energy is 2.2 kcal mol⁻¹ above that of *t*-1). The relaxed *t*-1 triplet energy was redetermined for this work for enhanced accuracy. The resulting value was 52.3 ± 0.9 kcal mol⁻¹ compared to 53.2 ± 2.4 kcal mol⁻¹ reported by Ni et al.^{19b} The corrected value of E_T is therefore 51.2 ± 0.9 kcal mol⁻¹ which leads to a value of Φ_{st} of 0.60 ± 0.03 with a 90% confidence limit.

Discussion

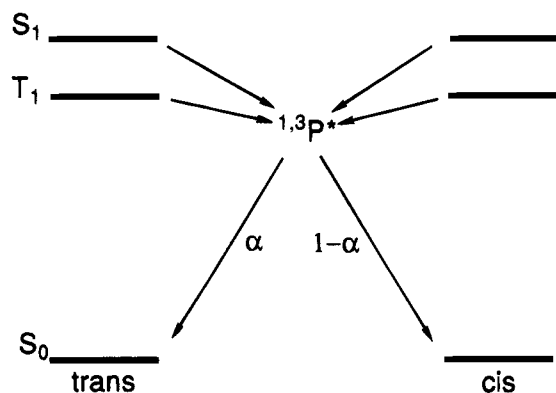
Electronic Spectra. The two lowest energy absorption bands of styrene have been assigned by analogy to the two lowest bands in benzene as arising from a forbidden 1L_b (${}^1B_2 \leftarrow {}^1A_1$ in C_{2v} symmetry) transition and an allowed 1L_a (${}^1A_1 \leftarrow {}^1A_1$ in C_{2v} symmetry) transition.^{10,12} With respect to benzene, the styrene

transitions are at longer wavelength and closer in energy, as would be expected for larger π systems. Aromatic substituents with π or nonbonding electrons also shift both transitions to lower energy. The presence of vibrational structure in the $S_1 \leftarrow S_0$ band is a strong indication that only limited structural reorganization occurs upon excitation into S_1 . Supersonic molecular jet spectroscopic studies showed this to be the case for styrene and established that both the ground and first excited singlet states possess a geometry in which the vinyl group is in the plane of the aromatic ring.^{8,9} The vibrational progression present upon excitation into S_1 was attributed to ring-localized stretching vibrations (ring-breathing).⁸ S_2 exhibits two vibrational progressions, assigned to the ethylenic double bond stretch and the phenyl–vinyl in-plane bend.⁷ The syn and anti conformers of *p*-methoxystyrene have been resolved in the vapor phase and have origins separated by 69 cm⁻¹.⁹ The presence of two conformers might result in broadening of the solution phase spectra of *t*-3, *t*-4, and *t*-6 in which the substituent can be either syn or anti to the double bond. The higher energy of the absorption maxima for *c*-1 vs *t*-1 was attributed by Fueno et al.¹⁰ to the nonplanarity of the *cis* isomer.

The fluorescence of styrene is assigned to emission from the 1L_b state.⁴ This assignment is consistent with the small Stokes shift between the lowest energy absorption band and fluorescence and the appearance of similar vibrational progressions in absorption and fluorescence. The fluorescence rate constants for all of the 1-arylpropenes (Table 2) are similar to that for styrene ($2.6 \times 10^7 \text{ s}^{-1}$)⁶ and significantly smaller than the value for *t*-S ($5.9 \times 10^8 \text{ s}^{-1}$).¹ The observation of smaller fluorescence quantum yields for S_2 vs S_1 excitation in several of the 1-arylpropenes (Table 2) indicates that internal conversion from S_2 to S_1 is not the exclusive decay pathway for S_2 in solution. No evidence for S_2 fluorescence has been reported for styrene or the 1-arylpropenes in the vapor phase, in solution, or in low-temperature glasses. Neither has phosphorescence been observed for styrene or the 1-arylpropenes in low-temperature glasses. The absence of phosphorescence in the case of styrene, *t*-1, and *c*-1 is attributed to barrierless torsion of the double bond on the triplet energy surface.^{19,20}

The appearance of the frontier molecular orbitals for *t*-1 (Figure 1) and the description of the two lowest energy transitions (Table 1) provided by the ZINDO calculations are essentially identical to those previously reported by Fueno et al.¹⁰ employing LCAO-SCF-CI calculations and by Hemley et al.¹³ employing CNDO/S-double CI calculations. All three calculations describe S_1 as arising from extensive configuration interaction dominated by the (HOMO – 1) to LUMO and HOMO to (LUMO + 1) transitions and S_2 as arising from a nearly pure HOMO to LUMO transition. ZINDO calculations for the 1-arylpropenes indicate that the substituents investigated do not significantly perturb the description of the two lowest energy singlet states (Table 1). These calculations also provide an explanation for the different effects of meta vs para substitution on the absorption spectra (Table 1). The absence of significant electron density on C-3 and C-5 of the aromatic ring in the HOMO and LUMO suggests that the presence of a substituent in these positions would not strongly affect the HOMO to LUMO ($S_2 \leftarrow S_0$) transition. Conversely, the $S_1 \leftarrow S_0$ transition possesses significant orbital coefficients at these positions from the mixing with the (HOMO – 1) and (LUMO + 1) transitions and would be expected to be sensitive to substituents appended meta to the double bond. By the same reasoning, substituents in the para positions would affect both the $S_1 \leftarrow S_0$ and the $S_2 \leftarrow S_0$ transitions, as all of the MO's involved possess contributions at that location. These trends

Scheme 1



are qualitatively reflected in the absorption and emission spectra, as the presence of a *m*-cyano substituent in *t*-3 shifts the weakly allowed $S_1 \leftarrow S_0$ absorption to longer wavelength while leaving the strongly allowed $S_2 \leftarrow S_0$ absorption unshifted (with respect to *t*-1). Since fluorescence emission occurs exclusively from S_1 , it is also shifted bathochromically. In contrast, placing the substituent in the para position (*t*-2) results in both absorption bands shifting to longer wavelengths.

Only small shifts in the absorption or fluorescence band maxima are observed in acetonitrile vs hexane solution. While this might appear to indicate that only a small degree of polarization is present in the lowest singlet excited state, Yates and co-workers²⁶ have suggested that the lowest singlet of styrene is highly polar or polarizable in order to account for both rapid protonation of the singlet state and measurements of transient electrochromism.

Isomerization. A generalized mechanism for singlet and triplet state photoisomerization is shown in Scheme 1. In the case of stilbene, the barriers for singlet state isomerization of both *trans* and *cis* isomers are sufficiently low to permit efficient formation of the twisted singlet intermediate (1P) at room temperature.^{1,2} This intermediate decays with nearly equal probability to the *trans* and *cis* ground states ($\alpha = 0.5$). The triplet states of both the stilbenes^{1,2} and the 1-arylpropenes^{19,20} also undergo essentially barrierless twisting to a perpendicular triplet (3P) which decays with equal probability to the ground states of *t*-1 and *c*-1 ($\alpha = 0.5$). In contrast the barrier for singlet state isomerization of *t*-1 is too high to permit efficient formation of a twisted singlet intermediate at room temperature.^{15,16} Rockley and Salisbury^{15a} attributed the moderately efficient isomerization of *t*-1 and *c*-1 in the vapor phase to intersystem crossing followed by isomerization on the triplet surface. Since intersystem crossing is generally an unactivated process it should be possible to distinguish singlet vs triplet mechanisms for the photoisomerization of 1-arylpropenes on the basis of the temperature dependence of the rate constant for isomerization (the triplet process being temperature independent and the singlet process being thermally activated). In addition to a difference in activation energies, the triplet pathway would be expected to have a much smaller preexponential factor than the singlet pathway since it involves a spin-forbidden process.²⁷

Singlet lifetimes and isomerization quantum yields for *c*-1 and *t*-1-*t*-6 were determined at low conversions of reactant to product isomer over a broad temperature range (Table 3). No corrections were made for the effects of changing pressure or

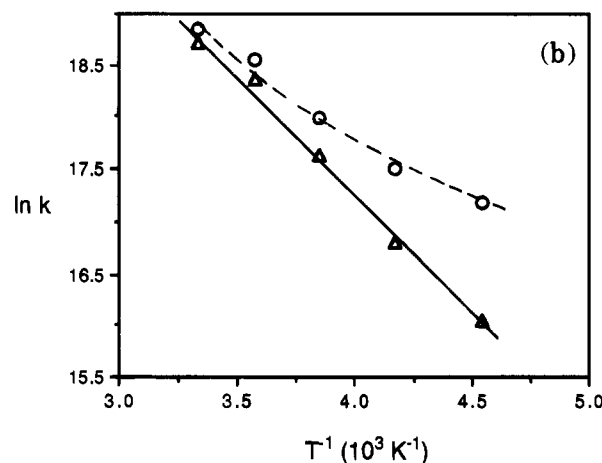
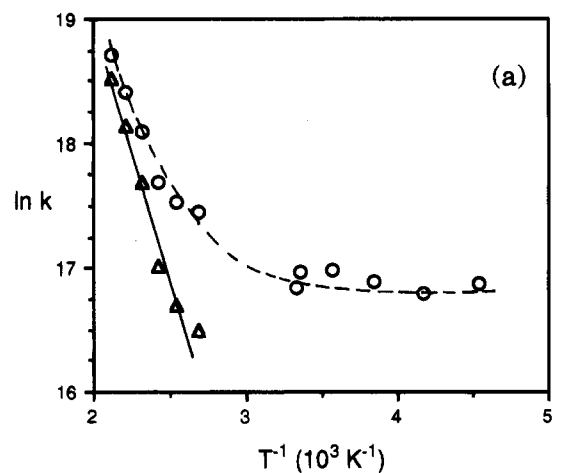


Figure 3. Arrhenius plots of the overall (O) and singlet (Δ) isomerization rates according to eq 3 for *t*-1 (a) and *c*-1 (b) in hexane solution.

viscosity with temperature, as these were judged to be insignificant over the temperature range of these experiments, or for singlet self-quenching. Since the lowest temperatures investigated (220 K in hexane and 235 K in acetonitrile) were well above the melting points of the solvents, a large increase in viscosity is not expected at low temperature. At the highest temperature employed (473 K), the vapor pressure of hexane is 18 bar. Only minor changes in the fluorescence quantum yield for *t*-S were observed by Brey et al.²⁸ over this range of pressure and viscosity. 1-Arylpropenes are expected to have lower volumes of activation than *t*-S, and thus should be less sensitive to changes in pressure and viscosity. Singlet self-quenching is not significant at the concentrations used ($\leq 10^{-3}$ M) for measurement of singlet lifetimes, fluorescence quantum yields, and intersystem crossing quantum yields for *t*-1. However, at the concentrations used for isomerization quantum yield measurements (10^{-2} M) approximately half of the *t*-1 singlets are subject to self-quenching. Self-quenching is less significant for *t*-6, which has a smaller self-quenching rate constant than that for *t*-1²³ and should also be less significant for 1-arylpropenes with shorter singlet lifetimes than *t*-1. The use of isomerization quantum yields which are not corrected for self-quenching for the calculation of isomerization activation parameters has little effect on the derived values.

Arrhenius plots of the rate constants for isomerization of *c*-1 and *t*-1-*t*-6 calculated assuming a singlet state mechanism (Scheme 1 with $\alpha = 0.5$, $k_1 = 2\Phi_1\tau_s^{-1}$) are shown in Figures 3-6 (broken curves). With the exception of the plot for *t*-4,

(26) (a) Wan, P.; Culshaw, S.; Yates, K. *J. Am. Chem. Soc.* **1982**, *104*, 2509. (b) Sinha, H. K.; Thomson, P. C. P.; Yates, K. *Can. J. Chem.* **1990**, *68*, 1507.

(27) Sun, Y.-P.; Saltiel, J.; Park, N. S.; Hoburg, E. A.; Waldeck, D. H. *J. Phys. Chem.* **1991**, *95*, 10336.

(28) Brey, L. A.; Schuster, G. B.; Drickamer, H. G. *J. Am. Chem. Soc.* **1979**, *101*, 129.

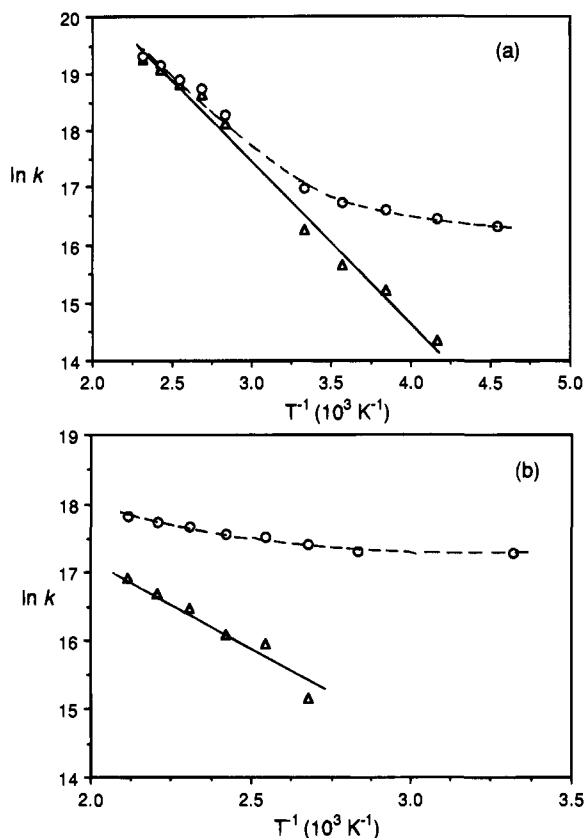


Figure 4. Arrhenius plots of the overall (O) and singlet (Δ) isomerization rates according to eq 3 for (a) *t*-2 and (b) *t*-3 in hexane solution.

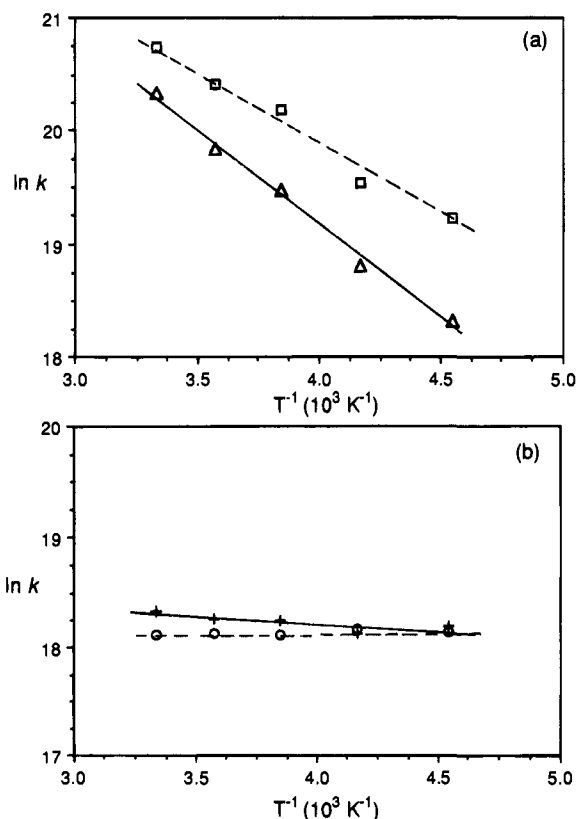


Figure 5. Arrhenius plots of (a) the singlet isomerization (Δ) rates and internal conversion rates (\square) for *t*-4 and (b) the overall isomerization rates (O) and fluorescence rates (+) for *t*-5 in hexane solution.

all of the plots exhibit varying amounts of curvature, attributed to the occurrence of competing singlet and triplet isomerization

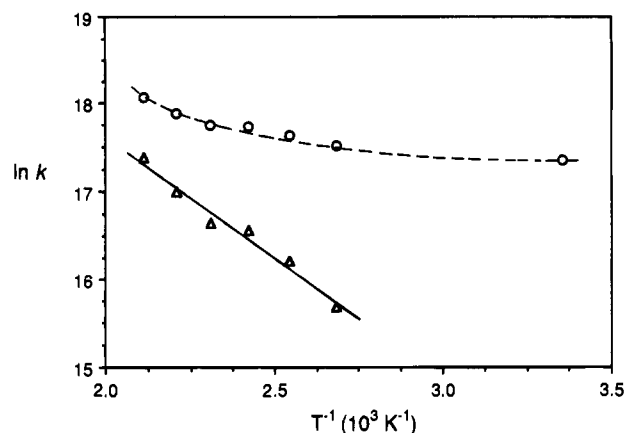


Figure 6. Arrhenius plots of the overall (O) and singlet (Δ) isomerization rates according to eq 3 for *t*-6 in hexane solution.

Table 4. Arrhenius Parameters for Isomerization of 1-Arylpropenes via the Excited Singlet State

| | E_a (kcal/mol) ^a | | log <i>A</i> | |
|-------------|-------------------------------|--------------|--------------|--------------|
| | hexane | acetonitrile | hexane | acetonitrile |
| <i>c</i> -1 | 4.6 | 4.8 | 11.5 | 11.9 |
| <i>t</i> -1 | 8.8 | 8.0 | 11.8 | 10.8 |
| <i>t</i> -2 | 5.6 | 2.6 | 11.6 | 11.1 |
| <i>t</i> -3 | 5.8 | 3.9 | 10.3 | 9.4 |
| <i>t</i> -4 | 3.3 | 3.1 | 11.5 | 11.4 |
| <i>t</i> -5 | >5 | >5 | | |
| <i>t</i> -6 | 5.6 | 4.2 | 10.4 | 10.1 |

^a Estimated error $\pm 15\%$.

pathways. It is possible to partition the overall isomerization quantum yield and rate constant into contributions from the singlet and triplet isomerization pathways using eqs 2 and 3, in which k_{is} and k_{st} are the rate constants for twisting from S_1 and intersystem crossing, respectively.

$$\Phi_i = 0.5k_{is}\tau_s + 0.5k_{st}\tau_s \quad (2)$$

$$k_{is} = 2\Phi_i\tau_s^{-1} - k_{st} \quad (3)$$

In order to extract values of k_{is} , it is first necessary to determine k_{st} . The latter may be directly measured for those compounds whose singlet isomerization pathway is not competitive at low temperatures ($k_{st} = 2k_i$) or left undetermined in cases where intersystem crossing does not appreciably contribute to isomerization ($k_{is} \cong k_i$). Intermediate cases may be analyzed using a differential form of the Arrhenius equation (eq 4) to obtain the activation energy associated with k_{is} and subsequently determine k_{st} .

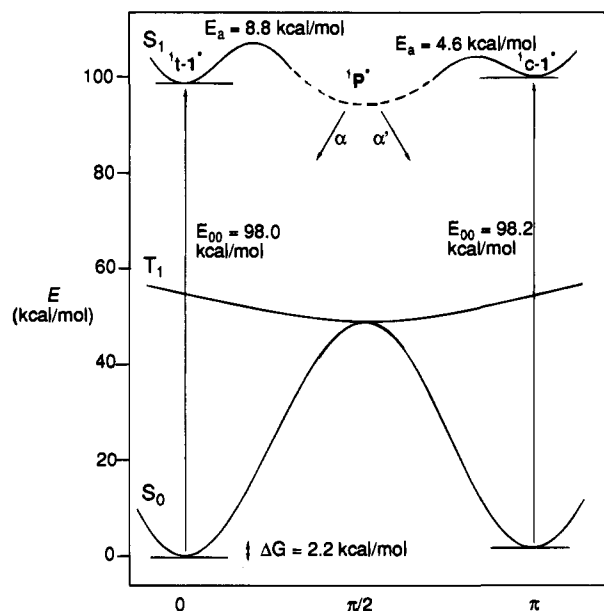
$$\ln\left(-\frac{dk_{is}}{dT^{-1}}\right) = \ln\left(A\frac{E_a}{R}\right) - \frac{E_a}{RT} \quad (4)$$

Arrhenius plots of $\ln(k_{is})$ vs T^{-1} for all of the 1-arylpropenes except *t*-5 are shown in Figures 3–6 (solid lines). Activation energies and preexponential factors obtained from linear least-squares analysis of these plots are reported in Table 4 and the calculated values for the temperature-independent rate constant for intersystem crossing in Table 5. The preexponential factors are somewhat lower than those reported for the singlet isomerization of *t*-S¹ but sufficiently large to support the conclusion that the temperature-dependent isomerization of the 1-arylpropenes occurs via a singlet state mechanism. The activation energies determined no doubt contain contributions arising from solvent-induced viscous drag, but those are expected to be small

Table 5. Rate Constants and Quantum Yields for Intersystem Crossing for the 1-Arylpropenes in Hexane and Acetonitrile Solution

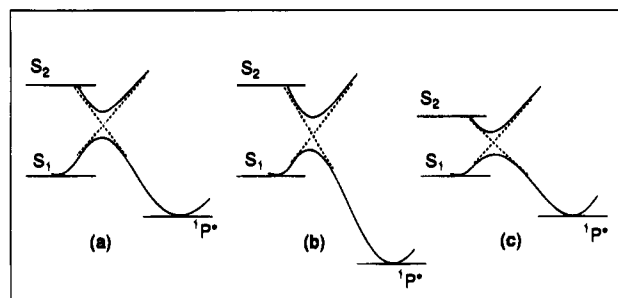
| | $10^{-7}k_{st}, s^{-1}$ | | Φ_{st} | |
|-----|-------------------------|---------------------------|--------------------------|---------------------------|
| | hexane ^a | acetonitrile ^a | hexane ^b | acetonitrile ^b |
| c-1 | 4.6 | 3.1 | 0.12 | 0.10 |
| t-1 | 4.6 (4.7) ^c | 3.1 | 0.58 (0.60) ^c | 0.34 |
| t-2 | 1.2 | <5 | 0.07 | ≤0.02 |
| t-3 | 3.6 | 4.8 | 0.34 | 0.54 |
| t-4 | <5 | <5 | <0.04 | <0.04 |
| t-5 | 13.2 | 20.0 | 0.50 | 0.52 |
| t-6 | 3.4 | 2.8 | 0.29 | 0.20 |

^a Values obtained from fitting of the temperature dependent isomerization data. ^b Values calculated from k_{st} and τ_s . ^c Values determined by PAC.

**Figure 7.** Potential energy diagram for twisting about the double bond of 1-phenylpropene in hexane in S_0 , S_1 , and T_1 . Dotted line indicates that the energy and geometry of $^1P^*$ are not known.

and similar for the entire series of compounds.²⁷ In the case of *t*-5, rate constants for singlet state isomerization could not be determined accurately due to unusually rapid intersystem crossing and thus an estimated lower limit of 5 kcal/mol for the singlet state isomerization is reported in Table 4. The Arrhenius plots for isomerization and fluorescence from *t*-5 both display very small slopes (Figure 5b).

The potential energy diagram for isomerization of *t*-1 and *c*-1 shown in Figure 7 can be constructed using our data for singlet state isomerization and the results of Caldwell and co-workers¹⁹ for triplet state isomerization. Singlet energies are estimated from fluorescence data (Table 2) and the ground state energy difference is obtained from the iodine-catalyzed equilibrium. The barriers for singlet state isomerization of *t*-1 and *c*-1 are significantly larger than those for the stilbenes, in accord with the longer singlet lifetimes for the 1-phenylpropenes vs the stilbenes. The energy of the perpendicular intermediate ($^1P^*$) is not known, but it is presumably lower than that of singlet *t*-1 or *c*-1. In the case of *t*-1 the barrier is sufficiently large to effectively prevent singlet isomerization at room temperature and below and hence isomerization occurs predominantly via intersystem crossing at these temperatures. However, at higher temperatures singlet state isomerization can compete with intersystem crossing. Bartocci et al.²⁹ have reported similar temperature dependence for the photoisomerization of *trans*-1-

**Figure 8.** Potential energy curves depicting the weakly avoided crossing between S_1 and S_2 [(a) after Bruni et al.¹¹] and the anticipated effects of stabilization of $^1P^*$ (b) and a decrease in the S_2-S_1 energy gap (c).

styrylnaphthalene and estimated the barrier for singlet isomerization to be ca. 10 kcal/mol. The barrier for *c*-1 is significantly smaller than that for *t*-1. As a consequence isomerization of *c*-1 at room temperature occurs predominantly (ca. 75%) via a singlet state mechanism.

The barrier for photoisomerization of styrene singlets is attributed to a weakly avoided crossing of the lowest singlet state (1L_b), whose energy increases with twisting about the ethylenic double bond, and either the second singlet state (1L_a) or a higher energy singlet state, whose energy decreases with twisting about the ethylenic double bond.^{8,11-14} A more weakly avoided crossing for *t*-1 vs *t*-S may be responsible for the smaller preexponential factor for isomerization of *t*-1.⁸ The effects of aromatic substituents and solvent polarity upon the barrier for styrene singlet isomerization can be analyzed using potential energy surfaces similar to that originally proposed by Bruni et al.¹¹ (Figure 8a). Substituents and polar solvents could lower the barrier for singlet state isomerization by either stabilizing $^1P^*$ with respect to S_1 (Figure 8b) or decreasing the S_2-S_1 energy gap (Figure 8c).

The nature of the twisted singlet ($^1P^*$) has been the subject of controversy among theoreticians, both zwitterionic (hole-pair)¹² and diradical¹³ lowest twisted singlet states having been proposed. The data in Table 4 indicate that both electron-withdrawing (*m*- and *p*-cyano and carbomethoxy) and electron-donating (methoxy) groups lower the barrier for singlet state isomerization. Since the preferred polarization of a zwitterionic styrene is expected to be (benzyl⁺ methyl⁻) on both theoretical¹³ and experimental²⁶ grounds, a methoxy group might have been expected to lower the activation energy more than a cyano group, contrary to observation. The effect of solvent polarity on *t*-1 is smaller than that for *t*-S.³⁰ The largest solvent effect is observed in the case of *t*-2 for which (benzyl⁺ methyl⁻) polarization should be least favorable. Taken together, these results would suggest that the transition state leading to the perpendicular intermediate possesses, at most, a small degree of polarization. *P*-Cyano, carbomethoxy, and methoxy substituents are also known to stabilize benzyl radicals whereas a *m*-cyano substituent destabilizes a benzyl radical.³¹ Thus the observed activation energies (Table 4) cannot be simply correlated with benzyl radical stabilities.

Both aromatic substituents and polar solvents can lower the S_2-S_1 energy gap (Figure 8c). While the energy of S_2 cannot be determined accurately from the solution spectra, both the observed gap between S_1 and the absorption maximum for S_2 and the calculated energy gap (Table 1) are smaller for *t*-4 than

(29) Bartocci, G.; Masetti, F.; Mazzucato, U. *J. Chem. Soc., Faraday Trans. 2* **1984**, *80*, 1093.

(30) Sivakumar, N.; Hoburg, E. A.; Waldeck, D. H. *J. Phys. Chem.* **1989**, *90*, 2305.

(31) Arnold, D. R. *NATO ASI Ser., Ser. C* **1986**, *189*, 171.

for the other 1-arylpropenes, in accord with its lower activation energy for singlet state isomerization (Table 4). The largest solvent-induced decrease in activation energy is observed for *t*-2, which also displays the largest solvent-induced decrease in the S_2 – S_1 energy gap. While these results indicate that the barrier for twisting on the S_1 energy surface is determined primarily by the S_2 – S_1 gap, other factors (e.g. stabilization of $^1P^*$, the curvature of the S_2 and S_1 energy curves, and the crossing twist angle) may influence the barrier. It is interesting to note that solvent-induced changes in the barrier height can result in a change in isomerization mechanism. Isomerization of *t*-2 at room temperature occurs predominantly via the triplet state in hexane solution and via the singlet state in acetonitrile solution. Bartocci et al.²⁹ observed a similar solvent effect on the relative importance of singlet vs triplet isomerization from styrylnaphthalenes in ethanol vs hexane solution.

The increase in isomerization efficiency and decrease in the quantum yield for fluorescence upon excitation at shorter wavelengths (into the S_2 absorption band) reported in Table 2 can be attributed to incomplete $S_1 \leftarrow S_2$ internal conversion. The potential energy surface shown in Figure 8a can account for these observations. Relaxation of planar S_2 to twisted S_2 may compete efficiently with internal conversion of planar S_2 to S_1 . Internal conversion of twisted S_2 would yield S_1 in its transition state geometry which could either relax to the planar fluorescent S_1 or to $^1P^*$. While incomplete internal conversion in solution is normally associated with molecules such as azulene which possess large S_1 – S_2 energy gaps, weak S_2 fluorescence with subpicosecond lifetimes has recently been detected for molecules such as β -carotene and diphenylacetylene for which the S_1 – S_2 energy gap is small.^{32,33} Salisbury and co-workers^{4,15} observed both inefficient fluorescence and isomerization upon S_2 excitation of *t*-1 in the low-pressure vapor phase and attributed these effects to rapid nonradiative decay pathways including fragmentation.

Intersystem Crossing and Internal Conversion. The quantum yield for intersystem crossing of *t*-1 determined by time-resolved photoacoustic calorimetry (PAC) is $\Phi_{st} = 0.60 \pm 0.03$. The value of Φ_{st} determined by PAC is similar to that obtained from the calculated value of k_{st} (Table 5) and the measured singlet lifetime ($\Phi_{st} = k_{st}\tau_s = 0.58$). These values can be compared to those obtained from the quantum yields for isomerization via the triplet state ($\Phi_{st} = 2\Phi_{it}$). Correction of the measured *t*-1 isomerization quantum yields (Table 2) for self-quenching provides calculated values of $\Phi_{st} = 0.50$ and 0.83 for 281 and 254 nm excitation, respectively. These values bracket the value measured by PAC using 266 nm excitation.

Our measured value of Φ_{st} for *t*-1 is larger than the values reported by Bonneau¹⁸ for styrene and *trans*-1-phenylbutene (0.40 and 0.13, respectively) based on triplet–triplet absorption measurements in cyclohexane solution. Since the optical absorption of styrene triplets is weak, it is possible that the use of high laser powers may have resulted in energy wasting by two-photon absorption. The singlet lifetime reported for *trans*-1-phenylbutene ($\tau_s = 4.3$ ns)¹⁸ is also significantly shorter than that for *t*-1, suggesting the possibility that self-quenching or impurity quenching shortened the singlet lifetime and lowered the triplet yield.

Intersystem crossing rate constants determined from the isomerization data and quantum yields for intersystem crossing in hexane and acetonitrile solution calculated from the estimated

rate constants and lifetimes of the 1-arylpropenes ($\Phi_{st} = k_{st}\tau_s$) are summarized in Table 5. Intersystem crossing does not compete effectively with singlet isomerization in the case of *t*-2 in acetonitrile solution and *t*-4 in hexane or acetonitrile solution. Based on the absence of curvature in the Arrhenius plot of k_i , an upper limit of 5×10^7 s⁻¹ can be estimated for the rate of intersystem crossing in these cases. Our calculated value of k_{st} for *t*-1 is slightly larger than the value for *t*-S estimated by Saltiel et al.¹ (3.9×10^7 s⁻¹). With the exception of *t*-5, the values of k_{st} for all of the 1-phenylpropenes are in the range 1 – 5×10^7 s⁻¹ and are not strongly solvent dependent. Thus the effects of substituents on the singlet lifetimes (Table 2) reflect changes in rate constants for singlet state isomerization and nonradiative decay rather than in the fluorescence or intersystem crossing rate constants. All of the 1-arylpropenes that we have investigated have lowest π,π^* states, as evidenced by both their fluorescence spectra and the results of ZINDO calculations. This is not the case for acetyl³⁴ and nitro²⁶ substituted styrenes which undergo rapid intersystem crossing and are nonfluorescent. The larger value of k_{st} observed for *t*-5 (1.3×10^8 s⁻¹) might reflect effective spin–orbit coupling between the trifluoromethyl substituent and the styrene chromophore.³⁵

The sum of the quantum yields for fluorescence and intersystem crossing of *t*-1 is 0.95 ± 0.05 . Thus internal conversion is not a significant process at or below room temperature. At higher temperatures the singlet lifetime of *t*-1 decreases with increasing temperature more rapidly than would be expected from the increase in the rate constant for isomerization (Table 3). This suggests the occurrence of thermally activated internal conversion as well as activated isomerization. Rate constants for activated internal conversion (k_{ic}) can be estimated by subtracting the sum of all the rates of processes leading to the decay of the excited state—the rates of fluorescence (k_f), singlet isomerization (k_{is}), and intersystem crossing (k_{st})—from the reciprocal of the singlet lifetime (eq 5).

$$k_{ic} = \tau^{-1} - (k_f + k_{is} + k_{st}) \quad (5)$$

Arrhenius plots of the resulting k_{ic} values for *t*-1 and *c*-1 are shown in Figure 9. In the case of *t*-1 the activation energy (9.6 kcal/mol) is slightly higher than that for singlet isomerization and the preexponential factor (1.1×10^{13} mol/s) is significantly higher than that for isomerization. As a consequence, internal conversion is expected to become the predominant decay pathway at high temperatures. In the case of *c*-1 the calculated activation energy (6.1 kcal/mol) and preexponential factor (2.6×10^{13} mol/s) are also much larger than those for isomerization. In those cases where intersystem crossing can be neglected (*t*-4, Figure 5a, and *t*-2 in acetonitrile), Arrhenius plots of k_{ic} are also linear and provide activation energies similar to those for isomerization and preexponential factors larger than those for isomerization.

The observation of barriers of similar magnitude for the thermally activated isomerization and internal conversion of *t*-1 and *c*-1 suggests that twisting about the styrene double bond may be related to the activated nonradiative decay process. Since the S_1 – S_2 surface crossing is weakly avoided and the preexponential for singlet isomerization is small, it is possible that internal conversion may compete effectively with surface crossing for vibrationally excited *t*-1 singlets. The potential energy surface for S_0 is expected to rise more rapidly with increased vibrational energy than the surface for S_1 . Thus the

(32) Shreve, A. P.; Trautman, J. K.; Owens, T. G.; Albrecht, A. C. *Chem. Phys. Lett.* **1991**, *178*, 89.

(33) Hirata, Y.; Okada, T.; Mataga, N.; Nomoto, T. *J. Phys. Chem.* **1992**, *96*, 6559. (b) Farrante, C.; Kensy, U.; Dick, B. *J. Phys. Chem.* **1993**, *97*, 13457.

(34) Tsubakiyama, K.; Miyagawa, K.; Kaizaki, K.; Yamamoto, M.; Nishijima, Y. *Bull. Chem. Soc. Jpn.* **1992**, *65*, 837.

(35) Janzen, E. G.; Gerlock, J. L. *J. Am. Chem. Soc.* **1967**, *89*, 4902.

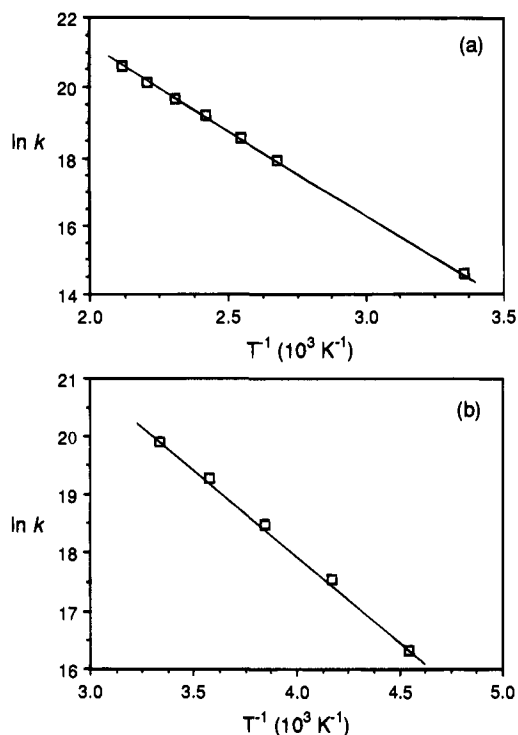


Figure 9. Arrhenius plots of the activated internal conversion k_{ic} according to eq 5 for (a) *t*-1 and (b) *c*-1 in hexane solution.

energy gap separating the two should decrease, rendering $S_0 \rightarrow S_1$ internal conversion more favorable with increasing vibrational energy.

Concluding Remarks. The behavior of the 1-arylpropenes differs from that of the stilbenes in several significant respects. The larger barrier for twisting on the singlet state results in longer singlet lifetimes and competition of intersystem crossing and internal conversion with fluorescence and isomerization from the singlet state. Only in the case of *c*-1 and *t*-4 are the barriers for twisting on the singlet state surface sufficiently low to permit isomerization to compete effectively with intersystem crossing at room temperature. The magnitude of the barrier for twisting on the singlet state surface is dependent upon aryl substitution and, in some cases, solvent polarity. These effects seem to be better correlated with the magnitude of the $S_2 \rightarrow S_1$ energy gap than the stability of either zwitterionic or biradical intermediates.

While we have not investigated the styrene singlet energy surface, Condirston and Laposa⁶ have reported that the styrene singlet lifetime is only modestly longer at 77 K vs 298 K (18.8 vs 14.6 ns). Thus it seems likely that the barrier for twisting on the singlet state surface is comparable to or larger than that for *t*-1. In contrast, we find that the singlet lifetime of 2-phenylpropene is significantly longer at 220 K vs 300 K (8.7 vs 1.9 ns). This increase in lifetime is similar to that for *c*-1 and suggests that the barriers for twisting on the singlet state surface are similar for 2-phenylpropene and *c*-1. The lower barrier for these styrene derivatives is probably related to nonbonded repulsion between the α - and *cis* β -methyl groups which results in nonplanar ground and singlet states.⁹

Experimental Section

Ultraviolet absorption spectra were obtained on a Hewlett-Packard 8452 A diode array spectrometer. Fluorescence spectra and lifetimes were recorded on a PTI LS-1 spectrometer using a pulsed xenon lamp or gated hydrogen arc lamp and single photon counting technique. The

decays were deconvoluted using a single-exponential or multiexponential least-squares analysis. The goodness of fit was judged by the reduced χ^2 value, as well as the randomness of the residuals and autocorrelation function. Hexane and acetonitrile were spectrophotometric grade (Aldrich) and used without further purification. *trans*-1-Phenylpropene (*t*-1, Aldrich) and *cis*-1-phenylpropene (Wiley Organics) were distilled prior to use. *trans*-(4-Methoxyphenyl)propene (Aldrich) was used as received. The synthesis of the remaining 1-arylpropenes has been reported elsewhere.³⁶ Compounds were analyzed on a Hewlett-Packard 5890 gas chromatograph equipped with a 10 m OV-1 0.54 mm i.d. capillary column and a flame ionization detector. Fluorescence quantum yields were determined relative to styrene ($\Phi_f = 0.24^6$) for solutions of matched absorbance (ca. 0.1 OD) at the excitation wavelength.

Room-temperature quantum yields for isomerization were determined in hexane or acetonitrile on an optical bench equipped with a 200 W high pressure mercury-xenon lamp and a Bausch & Lomb high intensity monochromator set at 280 nm. The solutions were contained in 10 mm thermostated and stirred quartz cuvettes, purged with nitrogen for 10–15 min, and irradiated to <5% conversion. The solutions were analyzed by GC and conversions compared to irradiated solutions of stilbene actinometer.³⁷ For temperatures below ambient, a nitrogen-cooled Oxford Instruments optical cryostat (DN 1704) and ITC four-temperature controller were used to maintain the sample temperature within ± 0.1 K of the desired value. A Teflon cannula was used both to introduce and remove samples for GC analysis and to permit mixing by slow purging with nitrogen during irradiation. The assembly was securely mounted on the optical bench for quantum yield measurements and in the sample compartment of the PTI LS-1 for the lifetime measurements. Measurements of singlet lifetimes and isomerization quantum yields at elevated temperatures required the construction of a heated stainless steel cell with a single sapphire window capable of withstanding high pressures. The cell heater was controlled by the ITC 4 controller, converted to use a chromel–alumel thermocouple and accurate to ± 0.5 K. Singlet lifetimes were recorded using the cell and a front face geometry with a 280 nm cut-off filter (Corning 0–53). Isomerization quantum yields were determined employing the same cell, mounted on the optical bench, and using a miniature magnetic stir bar to mix the sample during irradiation. No corrections were made for variations in the viscosity of the solvent with temperature, as these were judged to be small over the temperature range investigated.²⁸

Photoacoustic experiments utilized the 266 nm third harmonic output from a Continuum Model YG671C-10 Nd-YAG laser typically operated at 2 Hz (fwhm 5 ns), with incident powers in the 20–200 μ J range, and a front face photoacoustic cell with a 10 MHz transducer. The details of the experimental technique, cell design, and data analysis have been published previously.²⁴ Photoacoustic signals were collected as the average of 50 or 100 individual shots. Reported errors in quantum yield and lifetime measurements are 90% confidence limits of the mean values.

Acknowledgment. Financial support for this research has been provided by the National Science Foundation and in part by the Robert A. Welch Foundation. We thank Beth Yoon for determining the concentration dependence of the singlet lifetime and Jack Saltiel for enlightening discussions of styrene isomerization.

Supplementary Material Available: Absorption and fluorescence spectra of the 1-arylpropenes, photoacoustic data, and tables of temperature dependent singlet lifetimes, fluorescence quantum yields, and isomerization quantum yields (15 pages). This material is contained in many libraries on microfiche, immediately follows this article in the microfilm version of the journal, and can be ordered from the ACS; see any current masthead page for ordering information.

(36) Lewis, F. D.; Bassani, D. M. *J. Photochem. Photobiol. A. Chem.* **1994**, *81*, 13.

(37) Lewis, F. D.; Johnson, D. E. *J. Photochem.* **1977**, *7*, 421.